Highly efficient fluorescent chemosensor for nitro antibiotic detection based on luminescent coordination polymers with 2,6-di(4-carboxyphenyl)pyrazine

Shuang-Li Sun, [a] Xi-Yu Sun, [a] Qian Sun,[*a] and En-Qing Gao [b]

[a.] School of Chemistry and Molecular Engineering, East China Normal University, Shanghai, 200241, P. R. China. E-mail: xsun@chem.ecnu.edu.cn.

[b.] Shanghai key laboratory of Green Chemistry and Chemical Processes, School of chemistry and Molecular Engineering, East China Normal University, Shanghai 200062, P. R. China.

Table S1 selected **bond distance (Å) and angles (º) for the complexes 1-3 .**

Bond	**Bond length**		
	Cp（1）	**Cp（2）**	**Cp（3）**
M (1)-O (1)	2.0191(14)	2.1243(12)	2.050(2)
M (1)-O (2) #1	2.0972(13)	2.1428(13)	2.049(2)
M (1)-O (3) #2	2.1926(14)	2.2739(12)	2.125(2)
M (1)-O (4) #2	2.2162(14)	2.2656(12)	2.259(2)
M (1)-O (5)	2.0893(16)	2.1563(14)	2.092(2)
M (1)-N (2) #3	2.1995(15)	2.3423(14)	2.188(3)
Angles	**Angles (º)**		
O (1)-M (1)-O (5)	84.99(6)	84.21(5)	83.29(9)
O (1)-M (1)-O (2) #1	98.81(6)	101.81(5)	98.42(9)
O (1)-M (1)-O (3) #2	150.81(5)	148.95(5)	151.18(9)
O (5)-M (1)-O (2) #1	175.12(6)	169.67(5)	177.71(9)
O (5)-M (1)-O (3) #2	85.02(6)	85.25(5)	84.82(9)
O (2) #1-M (1)-O (3) #2	92.98(5)	93.42(5)	94.31(9)
O (1)-M (1)-N (2) #3	113.70(6)	115.56(5)	109.35(9)
O (5)-M (1)-N (2) #3	87.50(6)	83.95(5)	87.93(10)
O (3) #2-M (1)-N (2) #3	93.17(6)	92.19(5)	96.33(9)
O (2) #1-M (1)-N (2) #3	88.17(5)	85.86(5)	90.07(9)
O (1)-M (1)-O (4) #2	93.79(6)	96.54(5)	94.50(8)
O (5)-M (1)-O (4) #2	94.09(6)	94.34(5)	92.99(9)
O (3) #2-M (1)-O (4) #2	59.71(5)	58.03(4)	60.01(8)
O (2) #1-M (1)-O (4) #2	88.72(5)	91.41(5)	88.39(9)
N (2) #3-M (1)-O (4) #2	152.49(6)	149.92(5)	156.07(9)

Symmetry transformations used to generate equivalent atoms: #1 -x+2,-y+2,-z+2; #2 x+2,y+1,z+1; #3 x+1,y+1,z; #4 x-2,y-1,z-1; #5 x-1,y-1,z.

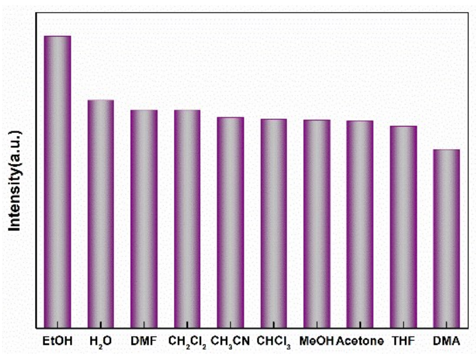

Fig. S1 Fluorescence emission intensities of **1** in different organic solvents and water.

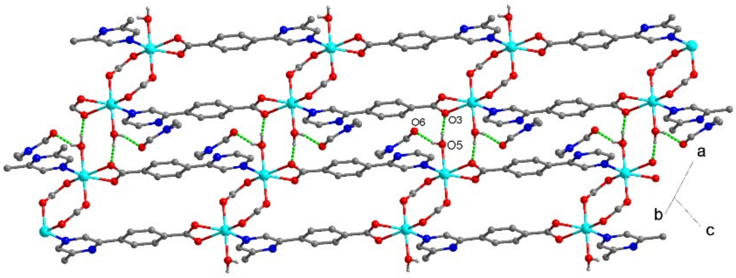

Figure S2 the hydrogen bonds between the layers, and the free DMF molecules bounded in the structure due to hydrogen bondings.

Table S2 Hydrogen bonding distance (Å) and angle (º) data

Complex	D-H...A	D-H	H...A	D...A	<DHA	Symmetry code
CP 1	O5-H5W1...O3A	0.81(3)	1.71(7)	2.666(6)	168.2(1)	A: 1-x, 1-y, 1-z
	O5-H5W2...O6B	0.75(4)	1.93(3)	2.669(9)	175.8(7)	B: 1+x, y, z
CP 2	O5-H5W1...O3A	0.90(4)	1.75(0)	2.654(2)	177.5(8)	A: 1-x, 1-y, 1-z
	O5-H5W2...O6B	0.74(1)	1.93(8)	2.673(7)	171.6(8)	B: 1+x, y, z
CP 3	O5-H5W1...O3A	0.95(2)	1.71(8)	2.666(7)	173.8(6)	A: 1-x, 1-y, 1-z
	O5-H5W2...O6B	0.76(3)	1.93(3)	2.669(9)	162.3(10)	B: 1+x, y, z

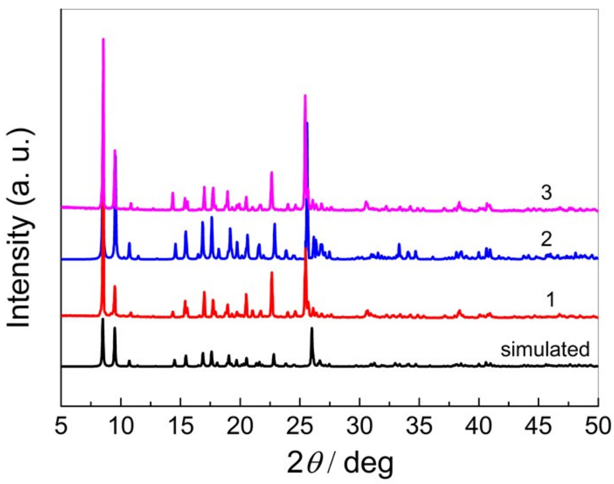

Fig. S3 the PXRD patterns of complexes **1**-**3**.

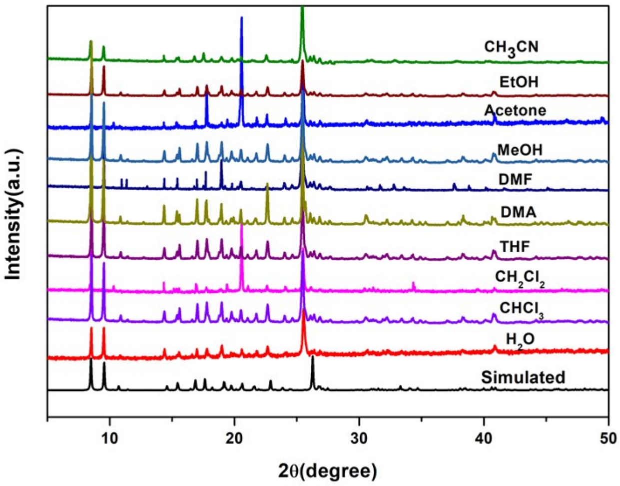

Fig. S4 the PXRD patterns of CP **1** in different different organic solvents and water. (After immersed for two hours)

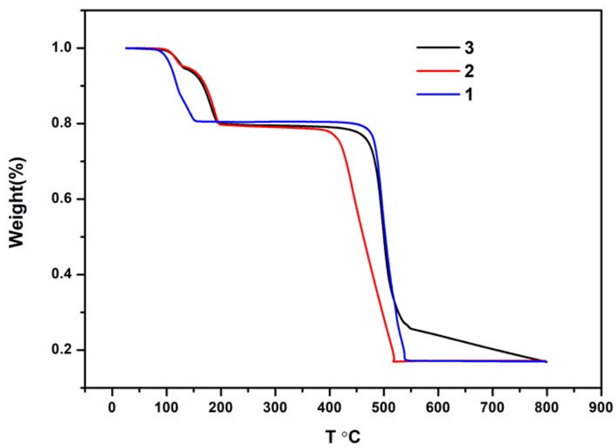

Fig. S5 TGA curves of CP **1-3**.

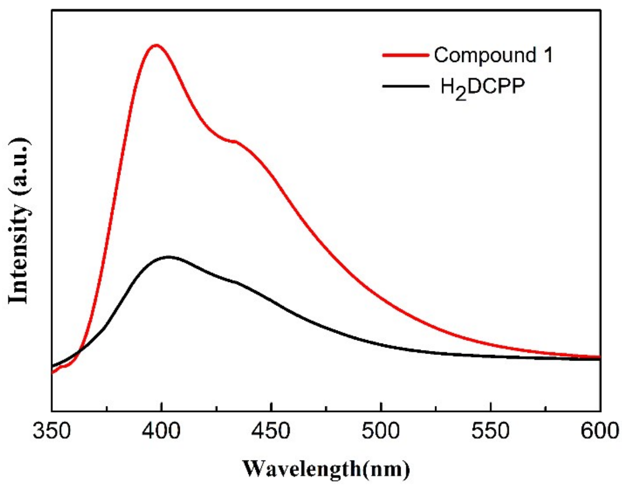

Fig. S6 The solid-state photoluminescence spectra of ligand (H_2DCCP) and the CP **1**.

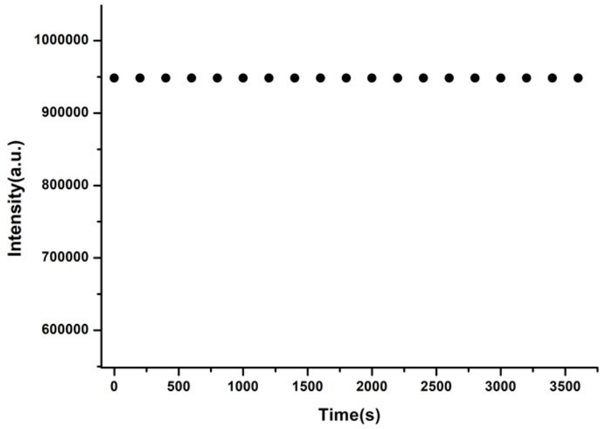

Fig. S7 A kinetic measurement of the emission intensity (at 408 nm) of the ethanol suspension of CP **1.**

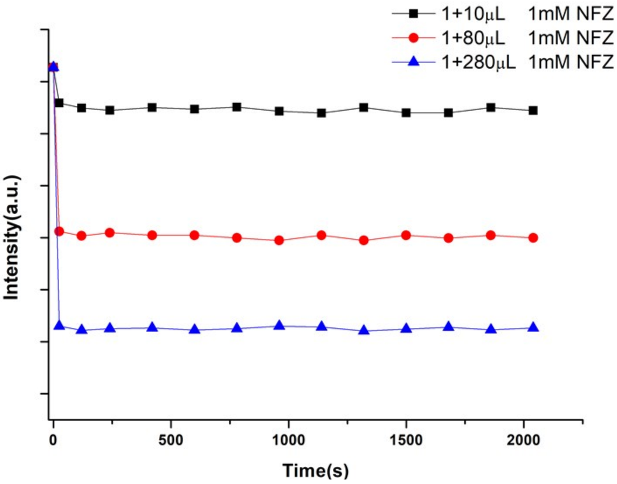

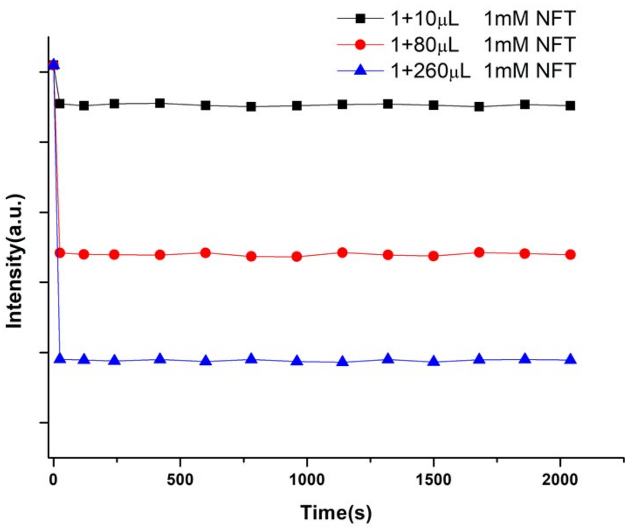

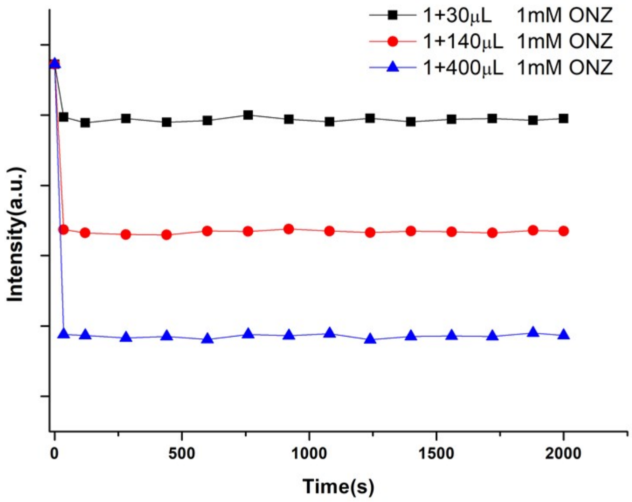

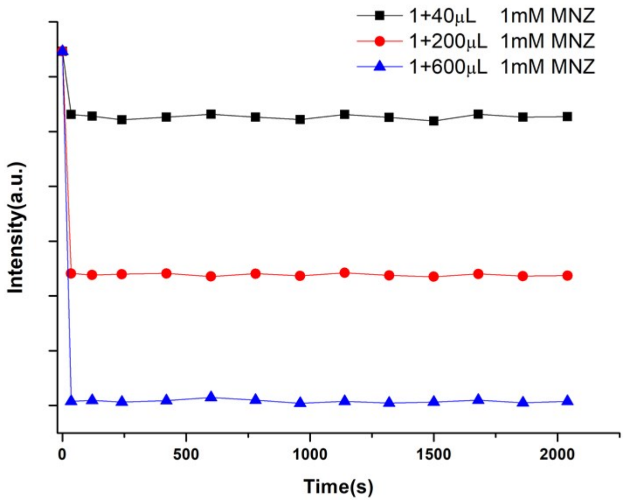

Fig. S8 Kinetic measurements of the emission intensity at 408 nm after adding NFZ NFT ONZ and MNZ to the ethanol suspensions of CP **1.**

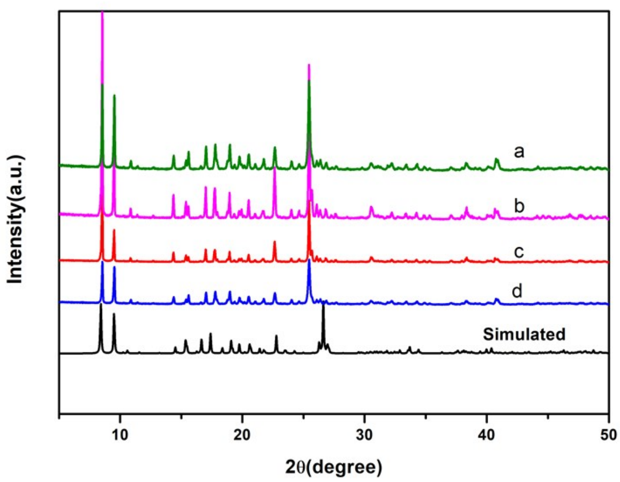

Fig.S9 PXRD patterns of CP **1** after 5 times repeatability experiments of (a) NFZ (b) NFT (c) ONZ and (d) MNZ.

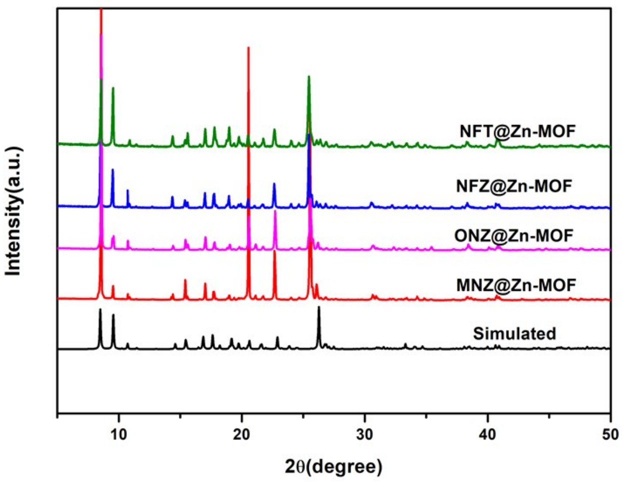

Fig. S10 PXRD patterns of CP **1** immersed in NFZ NFT ONZ and MNZ ethanol solutions. (After immersed for half an hour)

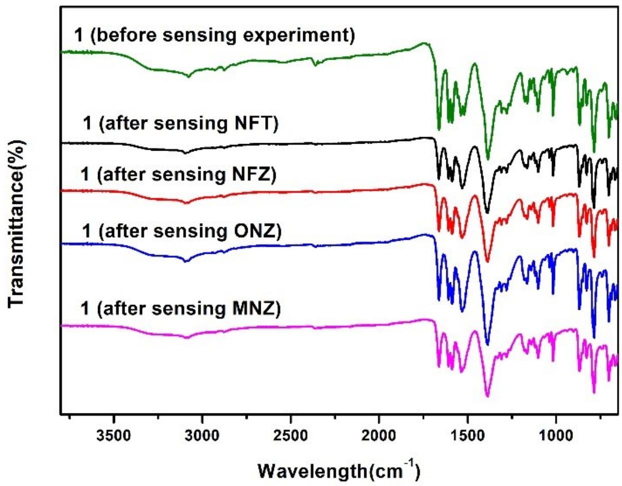

Fig. S11 FT-IR spectra of CP **1** before and after the detection of NFZ NFT ONZ and MNZ.

Table S3. Comparison of **1** with recent MOF-based luminescent sensors for NFZ NFT MNZ and ONZ.

MOF-based chemosensor	**Analyst**	**Linear range/μM**	**LOD /μM**	**Ksv×10⁴ /M⁻¹**	**Ref.**
$\{[Eu_2Na(Hpdbb)(pdbb)_2(CH_3COO)_2]\cdot 2.5DMA\}n$	NFZ	0-100	0.64	4.85	1
$\{[Eu_2Na(Hpdbb)(pdbb)_2(CH_3COO)_2]\cdot 2.5DMA\}n$	NFT	0-80	0.68	4.39	
$[Cd_2(L_2)(bpda)_2]\cdot 3DMF\cdot H_2O$	NFZ	0-30	1.27	3.1	2
$[Cd_2(L_2)(bpda)_2]\cdot 3DMF\cdot H_2O$	NFT	0-30	1.95	2.2	
$\{[Eu(H_2O)(BTCTB)]\cdot 2H_2O\}n$	NFZ	0-59	0.67	1.27	3
$\{[Eu(H_2O)(BTCTB)]\cdot 2H_2O\}n$	NFT	0-63	0.6	2.1	
$[(CH_3)_2NH_2][In(TNB)_{4/3}]\cdot(2DMF)(3H_2O)\supset DSM$	ONZ	0-500	——	1.08	4
$[(CH_3)_2NH_2][In(TNB)_{4/3}]\cdot(2DMF)(3H_2O)\supset DSM$	NFT	0-350	——	0.67	
$[Eu_2(2,3'\text{-}oba)_3(phen)_2]n$	MNZ	0.06-0.17	3.86	1.15	5
$[Pb_{1.5}(DBPT)]_2\cdot(DMA)_3(H_2O)_4$	MNZ	0-20	20	1.5	6
$[Tb(TATAB)(H_2O)]\cdot 2H_2O$	ONZ	0-80	0.171	1.62	7
$[Cd_3(DBPT)_2(H_2O)_4]\cdot 5H_2O$	ONZ	0-80	5	2.4	8
$[Cd_3(DBPT)_2(H_2O)_4]\cdot 5H_2O$	MNZ	0-80	10	2.0	
$[Eu(cppa)(OH)]\cdot xS$	ONZ	0-25	0.52	3.5	9
$[Eu(cppa)(OH)]\cdot xS$	NFT	0-25	0.43	2.33	
$Zr_6O_4(OH)_8(H_2O)_4(CTTA)_{8/3}$	ONZ	0-40	——	2.9	10
$Zr_6O_4(OH)_8(H_2O)_4(CTTA)_{8/3}$	NFT	0-40	——	3.8	
$Zr_6O_4(OH)_8(H_2O)_4(TTNA)_{8/3}$	ONZ	0-40	——	2.1	
$Zr_6O_4(OH)_8(H_2O)_4(TTNA)_{8/3}$	NFT	0-40	——	6.0	
MOF-76($Eu_{0.04}Tb_{0.96}$)	MNZ	0-150	1.02	2.95	11
$\{(Eu_2(TDC)_3(CH_3OH)_2\cdot(CH_3OH)\}n$	MNZ	0-60	0.51	2.81	12
$\{[Tb(H_2O)(BTCTB)]\cdot 2H_2O\}n$	MNZ	0-132	2.40	1.59	13
$[Zn(C_{18}N_2O_4H_{10})H_2O]\cdot DMF$	NFT	0-110	0.14	6.42	this work
$[Zn(C_{18}N_2O_4H_{10})H_2O]\cdot DMF$	NFZ	0-120	0.19	4.73	this work
$[Zn(C_{18}N_2O_4H_{10})H_2O]\cdot DMF$	ONZ	0-60	0.47	1.91	this work
$[Zn(C_{18}N_2O_4H_{10})H_2O]\cdot DMF$	MNZ	0-60	0.63	1.41	this work

H_2pdbb = 4,4'-(pyridine-2,6-diyl)dibenzolate, L_2 = 3,3',5,5'-tetra(1H-imidazol-1-yl)biphenyl; H_2bpda = 4,4'-carbonyldibenzoic acid, BTCTB= 3,3',3''-[1,3,5-benzenetriyltris(carbonylimino)]trisbenzoate, DSM= 4-[p-(dimethylamino)styryl]-1-ethylpyridi-nium, 2,3'-H_2oba = 2,3'-oxybis(benzoic acid), phen= 1,10-phenanthroline, H_3DBPT=3-(3,5-dicarboxylphenyl)-5-(4-carboxylphenyl)-1-H-1,2,4-triazole, H_3TATAB= 4,4',4''-s-triazine-1,3,5-triyltri-m-aminobenzoic acid, H_2cppa=5-(4-carboxyphenyl)picolinic acid, H_3CTTA = 5'-(4-carboxyphenyl)-2',4',6'-trimethyl-[1,1':3',1''-terphenyl]-4,4''-dicarboxylic acid, H_3TTNA = 6,6',6''-(2,4,6-trimethylbenzene-1,3,5-triyl)tris(2-naphthoic acid), H_2TDC = thiophene-2,5-dicarboxylate,

Table S4. HOMO and LUMO energy levels of different antibiotics calculated by density functional theory (DFT) at B3LYP/6-31G** accuracy level, using Gaussian 09 package of programs.

Analytes	HOMO(eV)	LUMO(eV)	Energy gap(eV)
NFZ	-6.316	-2.609	3.707
NFT	-6.578	-2.820	3.758
MNZ	-6.804	-2.256	4.548
SDZ	-6.238	-0.961	5.277
THI	-7.357	-1.294	6.063
TOB	-6.18	1.158	7.338
KAN	-5.687	1.401	7.088
ONZ	-6.916	-2.386	4.53
EM	-5.933	-0.153	5.78
MOF constituting linker(DCPP)	-6.642	-2.161	4.481

[1] S. Xu, J. J. Shi, B. Ding, Z. Y. Liu, X. G. Wang, X. J. Zhao and E. C. Yang, *Dalton Trans*, 2019, **48**, 1823-1834.

[2] Y.-L. Xu, Y. Liu, X.-H. Liu, Y. Zhao, P. Wang, Z.-L. Wang and W.-Y. Sun, *Polyhedron*, 2018, **154**, 350-356.

[3] H.-W. Yang, P. Xu, B. Ding, Z.-Y. Liu, X.-J. Zhao and E.-C. Yang, *Eur. J. Inorg. Chem*, 2019, **2019**, 5077-5084.

[4] H.-R. Fu, Y. Zhao, T. Xie, M.-L. Han, L.-F. Ma and S.-Q. Zang, *J. Mater. Chem. C*, 2018, **6**, 6440-6448.

[5] J.-M. Li, R. Li and X. Li, *CrystEngComm*, 2018, **20**, 4962-4972.

[6] Y. Sun, B. X. Dong and W. L. Liu, *Spectrochim Acta A Mol Biomol Spectrosc*, 2019, **223**, 117283-117290.

[7] J. H. Wei, J. W. Yi, M. L. Han, B. Li, S. Liu, Y. P. Wu, L. F. Ma and D. S. Li, *Chem Asian J*, 2019, **14**, 3694-3701.

[8] B. X. Dong, Y. M. Pan, W. L. Liu and Y. L. Teng, *Cryst.Growth Des.*, 2018, 18, 431-440.

[9] B. Li, Y. Y. Jiang, Y. Y. Sun, Y. J. Wang, M. L. Han, Y. P. Wu, L. F. Ma and D. S. Li, *Dalton Trans*, 2020, **49**, 14854-14862.

[10] B. Wang, X. L. Lv, D. W. Feng, L. H. Xie, J. Zhang, M. Li, Y. b. Xie, J. R. Li and H. C. Zhou, *J. Am. Chem. Soc.*, 2016,**138**, 6204-6216.

[11] Y. Yang, L. Zhao, M. Sun, P. Wei, G. Li and Y. Li, *Dyes and Pigments*, 2020, **180**,108444-108452.

[12] C. L. Li, F. Zhang, X. Li, G. W. Zhang, Y. Y. Yang, *J. Lumin*. 2019, **205**, 23–29.

[13] H.-W. Yang, P. Xu, X.-G. Wang, X.-J. Zhao and E.-C. Yang, *Z. Anorg. Allg. Chem.* 2020, **646**, 23-29.